Damping of Power Systems Oscillations using FACTS Power Oscillation Damper – Design and Performance Analysis

M. Mandour[1], M. EL-Shimy[2], F. Bendary[1] and W.M. Mansour[1]

[1]*Electric Power and Machines Department – Benha University, Egypt. Madel_ibec@yahoo.com*
[2]*Electric Power and Machines Department – Ain Shams University, Egypt. Shimymb@gmail.com*

***Abstract* – FACTS devices employ high speed, and high power semi-conductor technologies to help better regulate the power systems. To improve the damping of oscillations in power systems, supplementary control laws can be applied to the existing FACTS devices. These supplementary actions are referred to as power oscillation damping (POD) control. In this paper, the POD controllers are designed using the frequency response and residue methods. The small signal stability of power systems as affected by TCSC devices and PODs are evaluated and compared with the base power system where no FACTS devices are included. Both modal analysis and time domain simulations are presented to show the impact of the designed PODs on damping the electromechanical oscillations in power systems. Several examples are given to show the impact of POD input signals on the design and system response. The results show the capability of well designed FACTS-POD in improving the stability of power systems. In addition, the design is successfully implemented using the considered methods.**

Index Terms* – *FACTS; modal analysis; electromechanical oscillations; POD; time domain simulation.

I. Introduction

Power system stability has been recognized as an important problem for secure system operation since the 1920s [1]. The importance of this phenomenon has emerged due to the fact that many major blackouts in recent years caused by power system instability. As power systems have evolved through continuing growth in the interconnections and the increased operation in highly stressed conditions, different forms of power system instability have emerged [18].

The benefits of Flexible AC Transmission Systems (FACTS) devices are widely recognized by power system practitioners and the T&D community for enhancing both steady-state and dynamic performances of power systems [2-4]. The advent of these devices has required additional efforts in modeling and analysis, requiring engineers to have a wider background for a deeper understanding of power system's dynamic behavior.

The aim of this paper is to present procedures for designing power oscillation dampers (PODs) for FACTS devices in order to contextualize some important concepts of control theory into power system stability. A variety of design methods can be used for tuning POD parameters. The most common techniques are based on frequency response [5], pole placement [6], eigenvalues sensitivity [6, 7] and residue method [8].

Due to their popularity, POD designs are presented in this paper using the frequency domain and residue methods for control design. The Thyristor Controlled Series Compensator (TCSC) that belong to the family of FACTS devices is considered in this paper. TCSC are mainly used for power flow control and as active series compensators for AC power transmission lines. The small signal stability of power systems as affected by TCSC devices and PODs are evaluated and compared with the base power system where no FACTS devices are included. Both modal analysis and time domain simulation (TDS) are presented to show the impact of the designed PODs on damping the electromechanical oscillations in power systems. Several examples are given to show the impact of POD input signals on the design and system response.

II. The Study System, Modeling, and Modal Analysis

A. The Study System

The study system is shown in Fig.1. The system data are available at [9]. This system will be studied and analyzed with the aid of the *Power System Analysis Toolbox* (PSAT) version 2.1.7, the *Simulink* and the *control system toolbox* of Matlab 2012a [10-12]. The PSAT model of the system is shown in Fig. 2. Based on [9], the study system consists of four 555 MVA, 24 kV, 60 HZ units supplying power to an infinite bus through two transmission circuits as shown in Fig.1. The four generators are represented by one equivalent generator that is represented by the second order dynamic model [9, 10]. On 2220 MVA and 24 kV base, the transient reactance of the equivalent generator (x'_d) is 0.3 p.u, its inertia constant (H) is 3.5 sec, and its damping coefficient (D) is 10 in p.u torque/p.u speed. The initial conditions of the system in p.u on the 2220 MVA, 24 KV base are $\boldsymbol{E_B} = 0.995 \angle 0^o$, $\boldsymbol{E_t} = 1.000 \angle 36^o$, P = 0.9, and Q = 0.3 (overexcited).

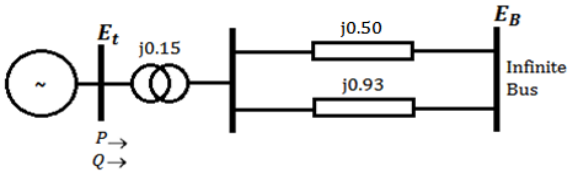

Fig. 1 The study system with the p.u network reactances are shown on 2220 MVA base

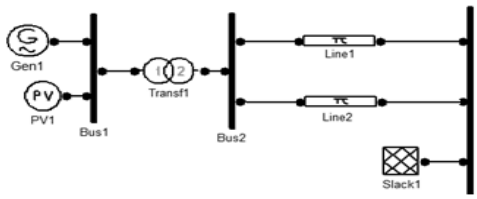

Fig. 2 The study system model in PSAT

B. Power system modelling and modal analysis

The power systems are dynamic systems that can be represented by differential algebraic equations in combination with non-linear algebraic equations. Hence, a power system can be dynamically described by a set of n first order nonlinear ordinary differential equations that are to be solved simultaneously. In vector-matrix notation, these equations are expressed as follows [9,19]:

$$\dot{x} = f(x,u) \quad (1)$$
$$y = g(x,u) \quad (2)$$

where: $x = [x_1, x_2 \cdots x_n]^t, u = [u_1, u_2 \cdots u_n]^t,$
$f = [f_1, f_2 \cdots f_n]^t, y = [y_1, y_2 \cdots y_n]^t, g = [g_1, g_2 \cdots g_n]^t$

n is the order of the system, r is the number of inputs, and m is the number of outputs. The column vector x is called the state vector and its entries are the state variables. The vector u is the vector of inputs to the system, which are external signals that have an impact on the performance of the system. The output variables (y) are those that can be observed in the system. The column vector y is the vector of system output variables, referred as output vector and g is the vector of nonlinear functions defining the output variables in terms of state and input variables.

The design of POD controllers is based on linear system techniques. After solving the power flow problem, a modal analysis is carried out by computing the eigenvalues and the participation factors of the state matrix of the system. The dynamic system is put into state space form as a combination of coupled first order, linearized differential equations that take the form,

$$\Delta\dot{x} = A\Delta x + B\Delta u \quad (3)$$

$$\mathrm{y} = C\Delta x + D\Delta u \quad (4)$$

where Δ represents a small deviation, A is the state matrix of size $n \times n$, B is the control matrix of size $n \times r$, C is the output matrix of size $m \times n$, and D is the feed forward matrix of size $m \times r$. The values of the matrix D define the proportion of input which appears directly in the output.

The eigenvalues λ of the state matrix A can be determined by solving $\det[A - \lambda I] = 0$. Let $\lambda_i = \sigma_i \pm j\omega_i$ be the i^{th} eigenvalue of the state matrix A; the real part gives the damping, and the imaginary part gives the frequency of oscillation. The relative damping ratio is then given by:

$$\xi_i = -\sigma_i / \sqrt{\sigma_i^2 + \omega_i^2} \quad (5)$$

If the state space matrix A has n distinct eigenvalues, then the diagonal matrix of the eigenvalues (Λ), the right eigenvectors (Φ), and the left eigenvectors (Ψ) are related by the following equations.

$$A\Phi = \Phi\Lambda \quad (6)$$
$$\Psi A = \Lambda\Psi \quad (7)$$
$$\Psi = \Phi^{-1} \quad (8)$$

In order to modify a mode of oscillation by a feedback controller, the chosen input must excite the mode and it must also be visible in the chosen output [8]. The measures of those two properties are the controllability and observability, respectively. The modal controllability $(\acute{B})$ and modal observability $(\acute{C})$ matrices are respectively defined by,

$$\acute{B} = \Phi^{-1}B \quad (9)$$
$$\acute{C} = C\Phi \quad (10)$$

The mode is uncontrollable if the corresponding row of the matrix $\acute{B}$ is zero. The mode is unobservable if the corresponding column of the matrix $\acute{C}$ is zero. If a mode is neither controllable nor observable, the feedback between the output and the input will have no effect on the mode.

C. TCSC Model

A TCSC as shown in Fig. 3(a) can be defined as capacitive reactance compensator which consists of a series fixed capacitor (FC) bank shunted by a thyristor-controlled reactor (TCR) in order to provide a smoothly variable series capacitive reactance. When placed in series with a transmission line as shown in Fig. 3(b), the TCSC can change the power flow on the line as a result of the changes made by the TCSC on the line reactance; the following algebraic equations approximately govern the power flow on a line connecting buses k and m (shown in Fig. 3(b)) when the line resistance is neglected.

$$P_{km} = V_k V_m (y_{km} + B_{TCSC}) \sin(\theta_k - \theta_m) = -P_{mk} \quad (11)$$

$$Q_{km} = V_k^2 (y_{km} + B_{TCSC}) - V_k V_m (y_{km} + B_{TCSC}) \cos(\theta_k - \theta_m) \quad (12)$$

$$Q_{mk} = V_m^2 (y_{km} + B_{TCSC}) - V_k V_m (y_{km} + B_{TCSC}) \cos(\theta_k - \theta_m) \quad (13)$$

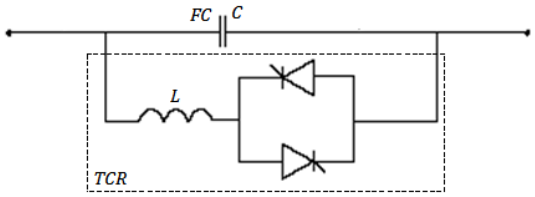

(a)

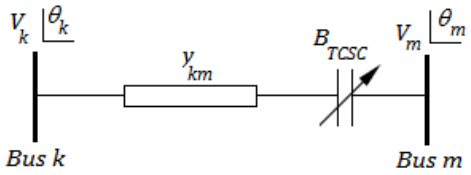

(b)

Fig.3 TCSC structure and control modes: (a) Basic structure, (b) A line with TCSC

The TCSC can be controlled to provide either a constant power control or a constant admittance control. The constant power control scheme is shown in Fig. 4(a). In this case, the state variables of the TCSC are $x_1 = x_c$ and $x_2 = \Delta P(K_I/s)$. Therefore, the state space model of the constant power regulator takes the form,

$$\dot{x}_1 = (K_r v_{POD} - x_{co} - x_1)/T_r \quad (14)$$

$$\dot{x}_2 = K_I \Delta P \quad (15)$$

where: $\Delta P = P_{km} - P_{ref}$, $x_{co} = K_P \Delta P + x_2$, $B(x_c) = C_p/\{x_{km}(1 - C_p)\}$, and $C_p = x_c/x_{km}$

The constant admittance regulator for TCSC takes the form shown in Fig. 4(b). In this case, one state variable ($x_1 = x_c$) represents the TCSC and the state space model takes the form,

$$\dot{x}_1 = (K_r v_{POD} - x_{cref} - x_1)/T_r \quad (16)$$

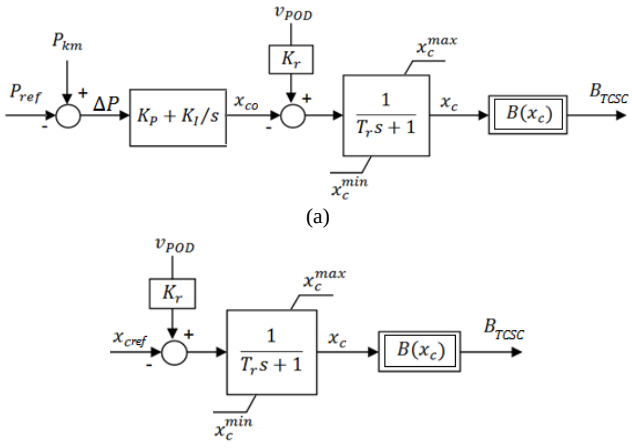

Fig. 4 Control modes of TCSC: (a) Constant power regulator; (b) Constant admittance regulator

The constant admittance operation of the TCSC will be considered for compensating differences between the reactances of two parallel transmission lines. The TCSC will be placed on line 2 shown in Fig. 2 and will be used to compensate the difference between the reactances of line 1 and line 2 of the study system shown in Fig. 1 and 2. The study system with the TCSC placed on line 2 is shown in Fig. 5. In this case, series compensation ratio is 0.462. The input variables to the PSAT block for modeling the TCSC are: T_r = 0.01 sec, x_{cmin} = 0.36 p.u, x_{cmax} = 0.373 p.u.

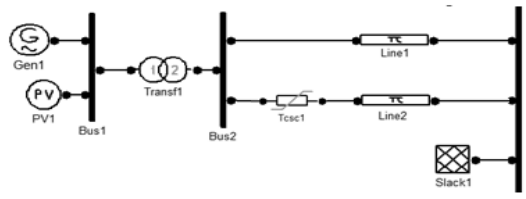

Fig.5 The study system after connecting the TCSC

III. POD Design

The POD controller is designed using two methods. These are the frequency response method and the residue method. The main design objective is to achieve a predefined damping level of the electromechanical oscillations. The general control diagram of the power system controlled by the POD is depicted in Fig. 6. As shown in Fig. 7, The structure of the POD controller is similar to the classical power system stabilizer (PSS). The controller consists of a stabilizer gain, a washout filter, and phase compensator blocks. The washout signal ensures that the POD output is zero in steady-state. The output signal v_{POD} is subjected to an anti-windup limiter and its dynamics are dependent on a small time constant T_r (in this paper T_r = 0.01 s). The gain K_w determines the amount of damping introduced by the POD and the phase compensator blocks provide the appropriate phase lead-lag compensation of the input signal.

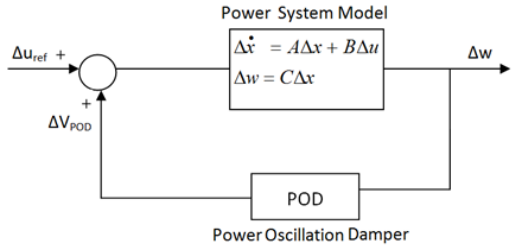

Fig.6 General feedback control system

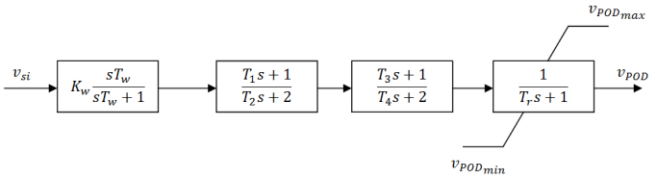

Fig.7: Scheme of the POD controller

A. *Frequency Response Method*

The POD controller is designed using the frequency response method through Nyquist plots of a given Open Loop Transfer Function (OLTF) [5].The Nyquist criterion allows to assess the closed-loop stability of a feedback system by checking the OLTF poles and plotting its frequency response [14,15]. Closed-loop stability of the open-loop unstable system is obtained by ensuring an anti-clockwise encirclement of the (-1) point of the complex plane in the Nyquist plot of the OLTF after applying feedback compensation [16, 17].

The main steps of the procedure for POD design using the frequency response method can be described by a flowchart as shown in Fig.8. As shown in Fig. 8, the main design steps in the POD design using the frequency response method can be summarized as follows [17]:

1) *Eigenvalue analysis:* In this design, the critical modes of the uncompensated system (i.e. without the POD) are identified based on eigenvalues and the participation factors of the state matrix. The participation factors (γ_{ij}) of the state variables to each eigenvalue are computed by using right and left eigenvectors. If Φ and Ψ represent respectively the right and the left eigenvector matrices

(Eqs. (6) to (8)), then the participation factor γ_{ij} of the i^{th} state variable to the j^{th} eigenvalue can be defined as [13]:

$$\gamma_{ij} = \Psi_{ij}\Phi_{ji}/\left(\Psi_j^t\Phi_j\right) \quad (17)$$

2) *State-space form:* In this step, all output and input matrices (A , B , C , and D) are determined. The observability and controllability as defined by Eqs. (9) and (10) can be determined based on these matrices.
3) *Nyquist analysis*: In this step, the value washout filter time constant is randomly selected between 1 and 20 Sec then the Nuquist plot of the uncompensated loop including the washout filter is constructed. The required phase compensation φ is then determined from the constructed Nyquist plot. The objective is to obtain a good phase margin based on the critical frequency ω_n.
4) *Compensator blocks tuning:* Based on the value of φ that is determined in the previous step, the parameters of the phase compensator blocks are determined in this step using [17],

$$\alpha = \{1 - \sin(\varphi/m_c)\}/\{1 + \sin(\varphi/m_c)\} \quad (18)$$
$$T_2 = 1/\omega_n\sqrt{\alpha} \quad (19)$$
$$T_1 = \alpha T_2 \quad (20)$$

where m_c is the number of the lead-lag blocks and ω_n is the frequency of the critical mode to be damped. The value of m_c is usually one or two; Fig. 7 shows a POD with two lead-lag blocks (i.e. m_c = 2) which is considered in this paper. In this layout, T_3 and T_4 are equal to T_1 and T_2.
5) *Damping ratio adjustment:* In this step, the root locus plot of the compensated system is used to determine the value of K_w that provide an acceptable damping ratio (i.e. $\xi \geq$ 10%). The POD design is completed by completing this step; however, further adjustment of the design can achieved by fine tunning the POD parameters as described in the next step.
6) *Fine tuning of the POD design:* The POD parameters have to be specified and chosen to fulfill specific performance parameters. The damping is one of the most important performance parameters; however, the performance is also goverened by many parameters such as the maximum rise time (t_r), the maximum overshoot (M_p), the desired damping ratio (ξ), and the settling time (t_s) [17]. The fulfillment of these performance parameters can be achieved by fine tuning of the POD parameters keeping in mind that the damping ratio is the main specification in power system control design and, for large power systems, 10% of damping is considered sufficient for POD controllers [9, 17].

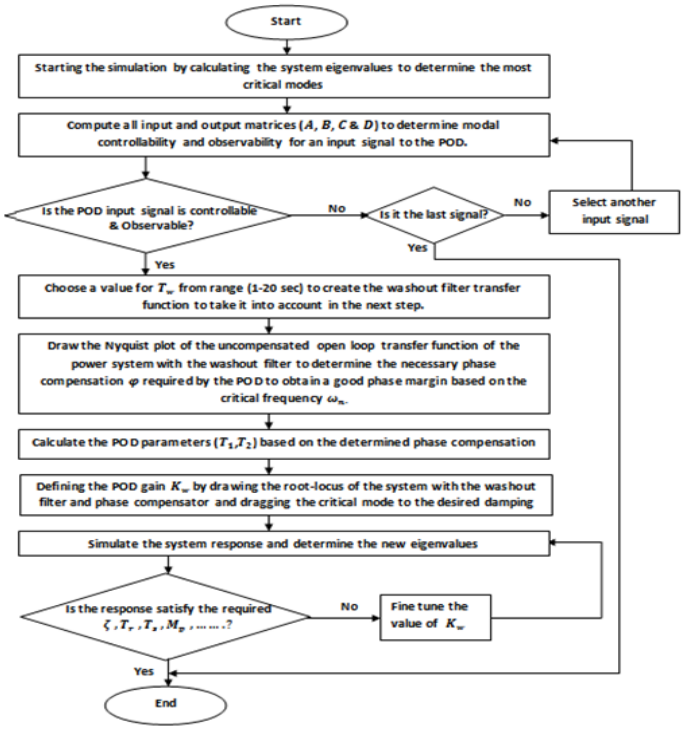

Fig. 8: Flowchart describing the frequency response method

B) Residue Method:

The residue method for POD design will be described based on the general feedback control system shown in Fig. 9. The transfer function of the system is $G(s)$ and the feedback control is $H(s)$. The open loop transfer function of a SISO system is [8]:

$$G(s) = \frac{\Delta y(s)}{\Delta u(s)} = C(sI - A)^{-1}B \quad (21)$$

$G(s)$ can be expanded in partial fractions of the Laplace transform in terms of the C matrix , the B matrix, the right eigenvectors, and the left eigenvectors as:

$$G(s) = \sum_{i=1}^{N} \frac{C\Phi(:,i)\Psi(i,:)B}{s - \lambda_i} = \sum_{i=1}^{N} \frac{R_i}{(s - \lambda_i)} \quad (22)$$

Each term in the nominator of the summation is a scalar called residue. The residue for a particular mode gives the sensitivity of the eigenvalue of that mode to the feedback between the output y and the input u of the SISO system. the residue is the product of the mode's observability and controllability.

When applying the feedback control, eigenvalues of the initial system $G(s)$ are changed. It can be proved [8] that when the feedback control is applied, movement of an eigenvalue is calculated by:

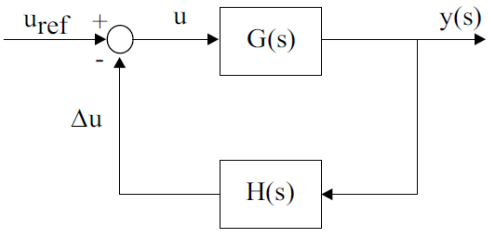

Fig.9 Closed-loop system with POD control.

$$\Delta\lambda_i = R_i H(\lambda_i) \quad (23)$$

It can be observed from (23) that the shift of the eigenvalue caused by a feedback controller is proportional to the magnitude of the residue. For improving the damping of the system, the change of eigenvalue must be directed towards the left half side of the complex plane. This is can be achieved by the use of the FACTS-POD controller. The compensation phase angle φ_{comp} required to move an eigenvalue to the left in parallel to the real axis is illustrated in Fig. 10. This phase shift can be implemented using the lead-lag function of the POD represented by Fig. 7 and equation (24). The parameters of the lead-lag compensator are determined using,

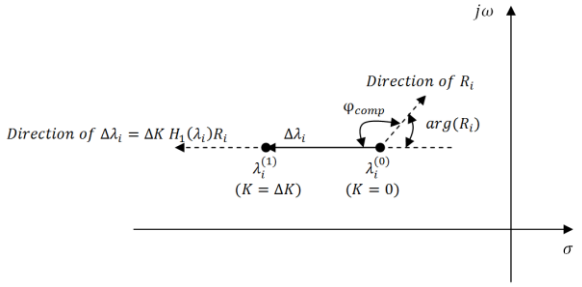

Fig.10 Shift of eigenvalues with the POD controller.

$$H(s) = K_w \frac{sT_w}{1+sT_w}\left[\frac{1+sT_1}{1+sT_2}\right]^{m_c} = K_w H_1(s) \quad (24)$$

$$\varphi_{comp} = 180^o - \arg(R_i) \quad (25)$$

$$\alpha_c = \{1-\sin(\varphi_{comp}/m_c)\}/\{1+\sin(\varphi_{comp}/m_c)\} \quad (26)$$

$$T_2 = 1/\omega_i\sqrt{\alpha_c} \quad (27)$$

$$T_1 = \alpha_c T_2 \quad (28)$$

where: $arg(R_i)$ is the phase angle of the residue R_i, ω_i is the frequency of the mode of oscillation in rad/sec, m_c is the number if compensation stages (in this paper, $m_c = 2$).

The controller gain K_w is computed as a function of the desired eigenvalue location $\lambda_{i,des}$ according to Eq. 24.

$$K_w = \left|\frac{\lambda_{i,des} - \lambda_i}{R_i H_1(\lambda_i)}\right| \quad (29)$$

The flowchart summarizing the previous design procedures is shown in Fig.11.

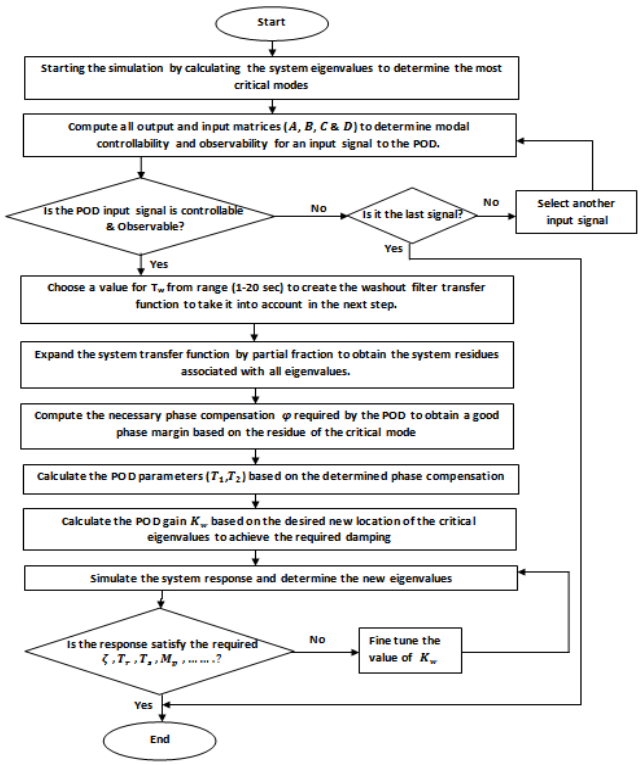

Fig.11 Flowchart describing the residue method

IV. Results and Disscussions

The results will be presented through studying the system described in Fig.1 in three scenarios as shown in Fig.12. In the Time Domain Analysis (TDS), the considered small-signal disturbance is a +10 % step increase in the mechanical power input (P_m) to the equivalent generator of the study system shown in Fig. 1, 2, and 4. The changes in the mechanical power will be started at t = 2 sec.

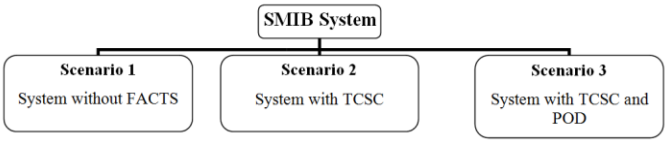

Fig.12 Study Scenarios

A) *Impact of the TCSC on the small- signal stability*

Tables I and II show the system dominant eigenvalues and their participation factors of scenario 1 and scenario 2 respectively.

TABLE I
SCENARIO 1 - DOMINANT EIGENVALUES AND PARTICIPATION FACTORS

Eigenvalues	f (Hz)	ξ (%)	Participation factors		Most Associated States
			δ_1	ω_1	
-0.71429 ± j7.6085	1.2163	9.34	0.5	0.5	δ_1, ω_1

TABLE II
SCENARIO 2 - DOMINANT EIGENVALUES AND PARTICIPATION FACTORS

Eigenvalues	f (Hz)	ξ (%)	Participation Factors			Most associated states
			δ	ω	X_{1_TCSC}	
-0.71429±j8.0854	1.2919	8.79	0.5	0.5	0	δ,ω
-100	0	100%	0	0	1	X_{1_TCSC}

It is clear from Tables I and II that both scenarios are stable; however, the eigenvalues of the system are changed as an effect of adding the TCSC to the system. The TCSC adds a non-oscillatory eigenvalue as depicted from Table II. The frequencies of the oscillatory modes of the system with TCSC are increased by 6.216% in comparison with the system without the TCSC while their damping ratios are reduced by 5.888%; (the percentage changes are calculated according to: % change = 100*(new value – old value)/old value). Therefore, the inclusion of the TCSC degrades the system stability. The damping ratio is less than 10%. Therefore, inclusion of POD is recommended to elevate the damping ratio to a value higher than or equal to 10% [9, 17]. POD designs according to the frequency response and residue methods are presented in the next sections; the objective is to increase the damping ratio to an acceptable value i.e. $\xi \geq 10\%$. Various input signals to the POD will be considered. In addition, the observability and controllability of them will be determined using equations (9) and (10).

B) Observability and controllability of various input signals

The observability and controllability of candidate feedback signals to the POD will be determined. Based on Fig. 1, these signals are the current across the transformer, the sending end active power, and the sending end reactive power. The modal controllability ($\acute{B}$) and modal observability ($\acute{C}$) matrices associated with the considered feedback signals are shown in Table III.

Table III
Modal observability and controllability of various feedback signals

Feedback signal	Modal observability C' matrix	Modal controllability B' matrix
The current across the transformer	$[1.3707 \quad 1.3707 \quad -0.2843]$	$\begin{bmatrix} -0.08 - j0.93 \\ -0.08 + j0.93 \\ 100 \end{bmatrix}$
The sending end active power	$[1.223 \quad 1.223 \quad -0.2785]$	
The sending end reactive power	$[0.1438 \quad 0.1438 \quad 0.0209]$	

Considering the critical electromechanical modes shown in Table II (highlighted by gray shading), it is depicted from Table III that all the considered signals are observable and controllable. Highest observability is associated with the current across the transformer feedback signal followed by the sending end active power then the sending end reactive power. Due to space limits, POD designs will be presented considering only the current across the transformer as a feedback signal; however, the presented design algorithms are general and can be applied to design PODs considering any acceptable feedback signal.

C) POD designs

Based on the flowcharts presented in Fig. 8 and 11, POD designs using the frequency response and residue methods are presented in this section. Designs with each of the considered feedback signals will be determined. Section IV-A and IV-B completed the initial stages of the design shown in Fig. 8 and 11 i.e. building the input and output matrices, analysis of the eigenvalues, modal controllability, and modal observability. The washout filter time constant (T_w) is chosen to be 7. This value is arbitrary selected between 1 and 20 [17].

1) The Frequency Response Method

With *the transformer current* as an input signal to the POD, the Nyquist plot (for positive frequencies) of the uncompensated OLTF (pre-design) and the compensated OLTF(post-design) is shown in Fig. 13.

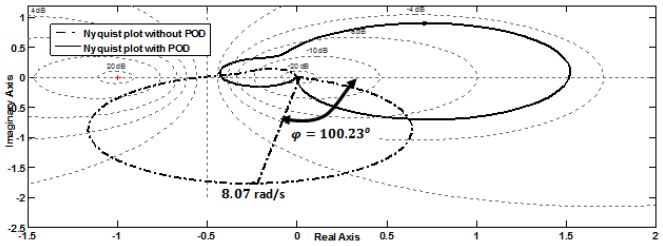

Fig. 13 Nyquist plots of SMIB system with and without POD

It is depicted from Fig. 13 and Table II that the OLTF for the system is stable, but presents poorly damped poles. For a good POD design, the resulting polar plot should be approximately symmetric with respect to the real axis of the complex plane [5, 17]. Based on the Nyquist plot shown in Fig. 13, the value of the angle φ required to relocate the critical frequency is 100.23°. Therefore, using equations (19) and (20), the parameters of the lead-lag compensators are T_1 = 0.3408 sec. and T_2 = 0.0449 sec. The gain K_w is determined based on the root locus of the system including the POD. The Matlab control system toolbox [12] is used to construct the root locus as shown in Fig. 14. The gain K_w is determined by dragging the critical mode to an acceptable damping ratio which is chosen to be higher than 10%. As shown in Fig. 14, the value of the damping of the critical mode in the compensated system is set to 15.63% and the corresponding gain is 0.0641. The transfer function of the POD is then takes the form

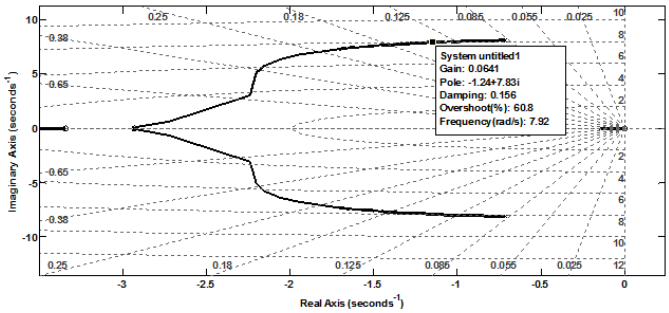

Fig. 14 Root locus of the compensated system and selection of the gain K_w

$$POD(s) = 0.0641\left[\frac{7s}{7s+1}\right]\left[\frac{0.3408s+1}{0.0449s+1}\right]^2 \qquad (30)$$

With the POD connected to the system shown in Fig. 5 as shown in Fig. 15, the design will be evaluated by both the eigenvalue analysis and the TDS of the compensated system. The results of the eigenvalue analysis of the compensated

system is shown in Table IV which indicates that the minimum damping of the system is improved to 15.63% as set by the POD design. Tables I and II show respectively that the damping of the system without TCSC is 9.34% and 8.79% in the uncompensated system with TCSC. This ensures the success of the POD design for improving the damping of the system.

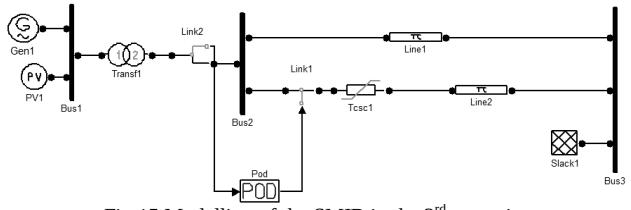

Fig.15 Modelling of the SMIB in the 3rd scenario

TABLE IV
FREQUENCY DOMAIN METHOD BASED EIGENVALUE ANALYSIS OF THE COMPENSATED SYSTEM

Eigenvalues	f (Hz)	ξ (%)	Most associated states
-12.3288 ±j61.9306	10.05	19.53%	X_{1_TCSC}, V_{3_POD}
-13.0749+j0	0	100%	V_{2_POD}
-1.2394±j7.8266	1.2612	15.63%	δ ,ω
-0.14262+j0	0	100%	V_{1_POD}

The TDS is performed considering a 10% step increase in the mechanical power input to the equivalent synchronous generator. This disturbance started at t = 2 sec. The simulation is performed using the Matlab control system toolbox. The responses of the systems of the three scenarios shown in Fig. 12 are compared as shown in Fig. 16.

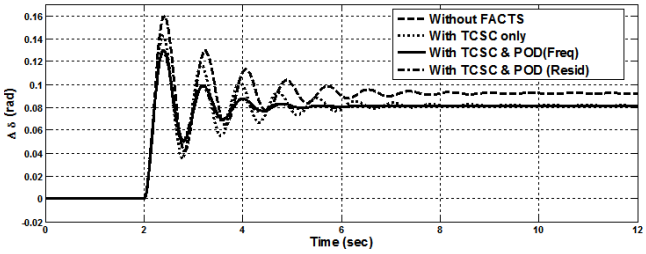

(a)

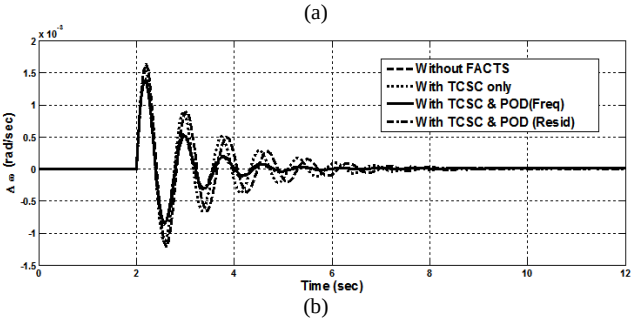

(b)

Fig. 16 TDS for 10% increase in the mechanical power: (a) Rotor angles; (b) Rotor angular speeds.

It is depicted from Fig. 16 that the POD improves the dynamic performance of the system through increasing the system damping, decreasing the overshoots, and decreasing the settling time.

2) The Residue Method

The design is based on the flowchart of Fig. 11. With *the transformer current* as an input signal to the POD, the residues for all eigenvalues of the system without POD should be obtained to determine the residue of the most critical mode. This is shown in Table IV. Afterward, the POD parameters can be determined as described in section III-B. The transfer function of the POD is then takes the form:

TABLE V
RESIDUES OF THE EIGENVALUES

Eigenvalues	Residues
-0.71429+j8.0854	-0.1043-j1.281
-0.71429-j8.0854	-0.1043+j1.281
-100	-28.4305

$$POD(s) = 0.0797\left[\frac{7s}{7s+1}\right]\left[\frac{0.2822s+1}{0.0542s+1}\right]^2 \quad (33)$$

Table V shows the eigenvalue analysis of the system after connecting the POD to the system which indicates the improvement in the system damping in comparison to the systems of scenarios 1 and 2. The TD responses as various scenarios subjected to the considered disturbance are shown in Fig. 16. The results validate the POD design using the residue method which results in approximately the same TD response of the system.

Table V
Residue method: Eigenvalue analysis of the compensated system

Eigenvalues	f (Hz)	ξ (%)	Most associated states
-30.7726 ±j42.5808	8.3614	58.57%	X_{1_TCSC}, V_{3_POD}
-1.2397±j7.9995	1.2884	15.33%	δ ,ω
-12.4271+j0	0	100%	V_{3_POD}
-0.14255+j0	0	100%	V_{1_POD}

3) Further Analysis

In this section a summary of some other related results will be presented to show the effect of some critical issues in damping of oscillations in power systems. These issues are the impact of POD input signal and the value of the time constant of the washout filter (T_w) on damping of power system oscillations. The impact of POD input signal is shown in Fig. 17 which indicates that better dynamic performance can be achieved with the transformer reactive power as a feedback signal while the other feedback signals (i.e. the transformer current and the transformer active power) have the same impact on the dynamic performance of the system. Therefore, careful choice of the input signal is important for damping maximization through POD design. High damping can be achieved with the transformer reactive power as an input signal because of the less control loop stability restrictions on the POD parameters in comparison with other signals.

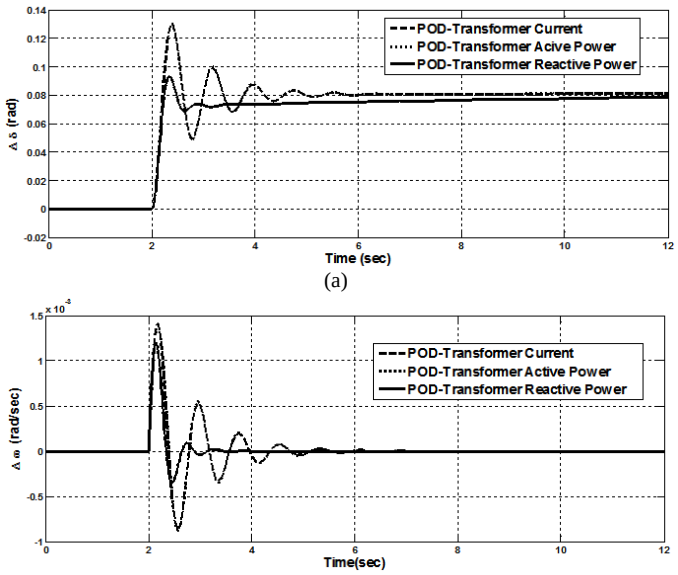

Fig. 17 TDS for 10% increase in the mechanical power with various feedback signals: (a) Rotor angles; (b) Rotor angular speeds.

The results shown in Table IV are obtained with T_w = 7. Although the literature recommended to select a random value for T_w between 1 to 20 sec, detailed analysis shows that the acceptable range of T_w is dependent on the system parameters and operating conditions. This is demonstrated in Table VI for the same design conditions shown in Table IV. Three values of Tw are shown. These values are 1 sec, 7 sec, and 14 sec.

TABLE IV
IMPACT OF T_w ON THE DYNAMIC PERFORMANCE

T_w = 1		T_w = 7		T_w = 14	
ξ (%)	*f* (Hz)	ξ (%)	*f* (Hz)	ξ (%)	*f* (Hz)
27.54%	9.5167	19.53%	10.05	**9.15%**	**10.2246**
100%	0	100%	0	100%	0
16%	1.2593	15.63%	1.2612	16.21%	1.2566
100%	0	100%	0	100%	0

Table IV shows that for all the considered values of T_w, the damping ratio of the critical electromechanical modes (shown in Table II) can be successfully increased to values higher than 15% which is practically acceptable damping level. The interesting part here is that, as shown in Table IV, that increasing Tw results in decreasing the damping ratios and increasing the frequencies of some of the electromechanical modes that was originally not critical (i.e. their damping ratio was higher than 10%). It is also shown that high value of T_w such as 14 as shown in Table IV could result in creating new critical modes in the compensated system. Therefore, careful selection of T_w should be considered in the initial stages of the design. It is also important to know that a suitable value of T_w for a specific system may be not suitable for another system. In addition, the impact of T_w on the dynamic performance is also sensitive to the operating conditions of a power system.

V. CONCLUSIONS

This paper presents a detailed analysis of the impact of TCSC on the dynamic performance of power systems. The results show that TCSC without POD reduces the dynamic stability. Therefore, POD is presented in this paper for improving the damping and stability of power systems. Two popular methods used for control design are successfully implemented for determining the parameters of POD. These methods are the frequency domain method and the residue method. The modal analysis as well as the time domain simulation verifies the results and show the dynamical benefits gained from the POD. In addition, critical design issues such as selection of the POD input signal and value of the time constant of the washout filter are also summarized. Since control of power system stability is an essential issue to keep power systems operating in a secure state. Therefore, further researches on POD design improvement are recommended for future work.

REFERENCES

[1] P. Kundur, V. Ajjarapu, G. Andersson, A. Bose, C. Canizares, N. Hatziargyriou, D. Hill, A. Stankovic, C. Taylor, T. V. Cutsem and V. Vittal, "Definition and classification of power system stability ieee/cigre joint task force on stability terms and definitions", IEEE Transactions on Power Systems, Vol.19, No.3, Aug. 2004.

[2] J. J. Paserba, "How FACTS controllers benefit AC transmission systems," presented at the IEEE Power Engineering Society General Meeting, Denver, CO, 2004.

[3] Y. H. Song and A. T. Johns, Flexible AC Transmission Systems (FACTS). London: The Institution of Electrical Engineers, 1999.

[4] N. G. Hingorani and L. Gyugyi, Understanding FACTS: Concepts and Technology of Flexible AC Transmission Systems. New York: Institute of Electrical and Electronics Engineers, 2000.

[5] N. Martins and L. Lima, "Eigenvalue and Frequency Domain Analysis of Small-Signal Electromechanical Stability Problems," IEEE Symposium on Application of Eigenanalysis and Frequency Domain Method for System Dynamic Performance, 1989.

[6] B. C. Pal, "Robust pole placement versus root-locus approach in the context of damping interarea oscillations in power systems," IEE Proceedings on Generation, Transmission and Distribution, vol. 149, Nov 2002.

[7] R. Rouco and F. L. Pagola, "An eigenvalue sensitivity approach to location and controller design of controllable series capacitors for damping power system oscillations," IEEE Transactions on Power Systems, vol. 12, Nov 1997.

[8] R. Sadikovic, et al., "Application of FACTS devices for damping of power system oscillations," presented at the IEEE Power Tech, St. Petersburg, Russia, June 2005.

[9] P. Kunder, Power system stability and control. New York: McGraw-Hill, 1994.

[10] F. Milano. PSAT version 2.1.7 Available: http://www3.uclm.es/profesorado/federico.milano/psat.htm

[11] F. Milano, "An Open Source Power System Analysis Toolbox" IEEE Transactions on Power Systems," IEEE Transactions on Power Systems, vol. 20, Aug 2005.

[12] I. The MathWorks. MATLAB and Simulink R2012a. Available: http://www.mathworks.com

[13] F. Milano, Power System Analysis Toolbox – Documentation for PSAT Version 2.0.0, Feb 2008.

[14] N. Martins, et al., "Using a TCSC for line power scheduling and system oscillation damping-small signal and transient stability studies," presented at the IEEE Power Engineering Society Winter Meeting, 2000.

[15] G. F. Franklin, et al., Feedback Control Of Dynamic Systems, 4 ed. New Jersey: Prentice Hall, 2003.

[16] R. C. Dorf and R. H. Bishop, Modern control systems, 9 ed. Upper Saddle River, New Jersey: Prentice-Hall, 2001.

[17] H. M. Ayres, I. Kopcak, M. S. Castro, F. Milano and V. F. d. Costa, "A didactic procedure for designing power oscillation damper of facts devices", Simulation Modelling Practice and Theory, vol.18, no.6 June 2010.

[18] H. Hongyang, Z. Xu, and W. Hua, "Estimation of interarea modes in large power systems." *International Journal of Electrical Power & Energy Systems* 53 (2013), pp. 196-208.

[19] C.E. Ugalde-Loo, E. Acha, and E Licéaga-Castro. "Multi-machine power system state-space modelling for small-signal stability assessments." *Applied Mathematical Modelling* 37, no. 24 (2013), pp. 10141-10161.